

Dynamic Characteristics of a Centrifugal Blood Pump with Conical Spiral Groove Bearings

Yoichi Nakamura and Hiroshi Tsukamoto

Graduate school of life science and systems engineering, Kyushu Institute of Technology
2-4, Hibikino, Wakamatsu-ku, Kitakyushu, Fukuoka, 808-0196, Japan

tsukamoto@life.kyutech.ac.jp, nakamura-youichi@edu.life.kyutech.ac.jp

Abstract

This paper describes the dynamic characteristics of a centrifugal blood pump with hydrodynamic levitating bearings. Flow fluctuations were realized from 0.25 to 3.0 Hz by an oscillator driver in the fluid circulatory system for the test pump with conical spiral groove bearings. The stability test was done for the whirling motion of impeller and the pump stability was discussed based on the dynamic tests under sinusoidal change in flow rate. The measured impeller whirling motions were found to be stable, and the response of pump total pressure rise to flow rate change was also stable for the test pump.

1. INTRODUCTION

Blood pumps have come to the front as the therapeutic instrument for serious heart failure. The centrifugal pump may be superior among many types of blood pumps because of its compact and easily-controlled structure. Advanced centrifugal blood pumps have equipped with the magnetically levitated bearing [1, 2, 3] or hydrodynamic levitated bearing [4, 5, 6] for the suppression of thrombus. Those pumps are affected by pulsation flow when they are set downstream of living heart as the ventricular assist device (VAD). Therefore, the dynamic characteristics of those blood pumps should make clear under flow fluctuation. Dynamic characteristics of turbopumps have been investigated intensively for the case in which the flow rate oscillates periodically about mean operating point with small amplitude. In this case, the pump performance can be described by a transfer matrix representation to relate the quantities at the suction and discharge of the pump (Brennen [7]). Anderson et al. [8], and Ng and Brennen [9], have contributed to such a description. Yoshino and Akamatsu [1] clarified the dynamic characteristics of blood pump with magnetically levitated bearing. However, the stabilities of the blood pump with hydrodynamic levitated bearing have not been clear under the variable load in unsteady operations. In this paper the stabilities were discussed experimentally for the pump under whirling motion in sinusoidal change in flow rate.

2. TEST PUMP

Figure 1 shows the cross sectional view and coordinate system of the test pump in the present study [10]. Here, ε : eccentricity of rotor center ($\varepsilon = \sqrt{x^2 + y^2}$), σ : standard deviation of ε , Ω : angular velocity of whirling motion, and ω : angular velocity of rotor. The test impeller was designed so as to satisfy the specification of VAD. The test pump rotor of diameter 40 mm and length 84 mm comprises conical spiral groove bearing (CSGB), magnet coupling, rotor, and pump casing. The CSGB geometry was determined by Muijderman's experimental formula [11] and preliminary test results [10]. The impeller geometry was determined so that the blade-to-blade passage areas may be kept as constant as possible for the prevention of hemolysis. The test pump was manufactured in materials of acrylic resin using Rapid Prototyping technology.

Dynamic Characteristics of a Centrifugal Blood Pump with Conical Spiral Groove Bearings

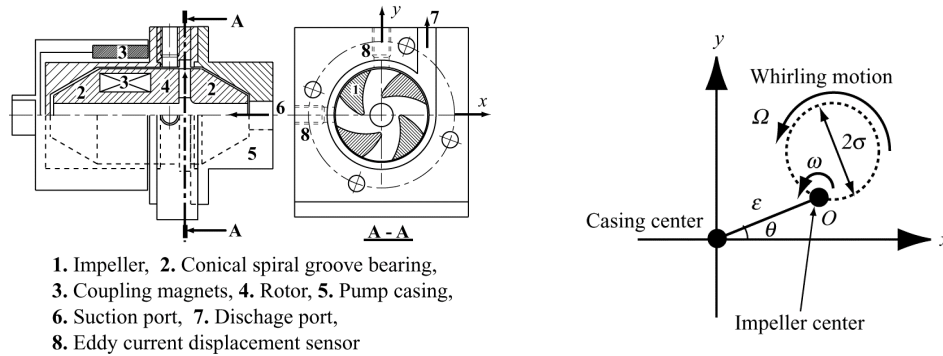


Fig. 1 Cross sectional view and coordinate systems of test pump and impeller.

3. EXPERIMENTAL METHODOLOGY

Figure 2 shows the schematics of the experimental setup for dynamic characteristic tests. The test pump was driven by an inverter controlled 0.2 kW induction motor through the magnet coupling. The water flows in the test pump from the reservoir through the pressurized chamber equipped with the oscillator driver, and returns the reservoir through the electromagnetic flow meter and control valve. The displacement of the rotor was measured in the x - y coordinates of its rotating center using an eddy current displacement sensor. The rotational speed of the pump rotor, n ($=\omega/2\pi$), was measured by a photo-electric tachometer. Sinusoidal change in flow rate was given around the flow rate set by the control valve using a sliding piston in a pressurized chamber. The sliding piston was driven by a geared motor (gear ratio $1/5$, 0.2 kW) with a slowdown mechanism and caused sinusoidal change in flow rate. The fluctuation frequency, f , was chosen from 0.25 to 3.0 Hz so as to correspond to the heartbeat of the living body.

Figure 3 presents an example of the time histories of measured instantaneous suction and discharge pressure, p_s and p_d , volumetric flow rate Q , and impeller center coordinate at casing, in which flow rate were excited with the frequency $f = 1.0\text{ Hz}$ around the rated operating condition ($\phi/\phi_D = 1.0$, and $n = 3000\text{ min}^{-1}$). All variables fluctuate around their mean values designated by suffix θ as can be seen in this figure. The measured data were processed to get the frequency response of variables to flow rate in the manner similar to Tsukamoto et al. [12]

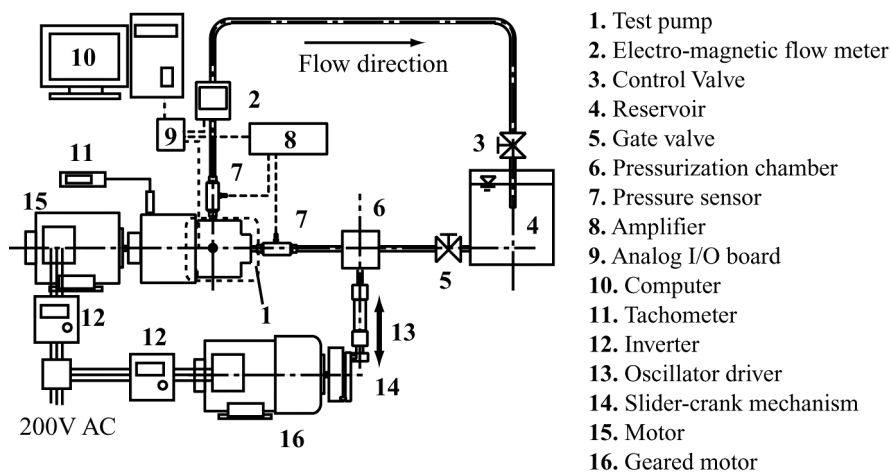


Fig. 2 Schematics of experimental setup and measurement instruments.

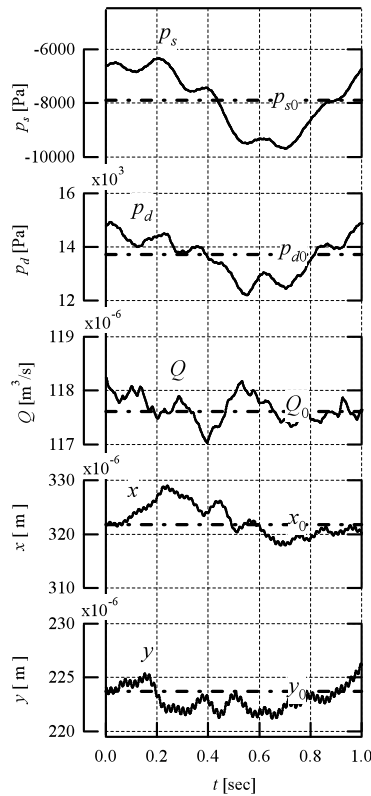


Fig. 3 Time histories of p_s , p_d , Q , x , and y ($\phi/\phi_D = 1.0$, $n = 3000 \text{ min}^{-1}$, $f = 1.0 \text{ Hz}$).

4. PUMP TRANSFER MATRIX OF CENTRIFUGAL PUMP

The pressure and flow pulsations at pump suction and discharge are connected by the following 2×2 complex transfer matrix for noncavitating pump [13].

$$\begin{pmatrix} p_d / \rho g \\ Q \end{pmatrix} = \begin{pmatrix} 1 & -Z_p \\ 0 & 1 \end{pmatrix} \begin{pmatrix} p_s / \rho g \\ Q \end{pmatrix} \quad (1)$$

where Z_p is the complex impedance of pump, which is divided into pump resistance $Re(Z_p)$ and pump inductance $Im(Z_p)$. At low frequency where quasi-steady change approximation is valid, the pump impedance can be approximated by the following nondimensional form Z_p^* :

$$Z_p^* = \frac{A_2 g}{u_2} Z_p = -\frac{A_2 g}{u_2} \frac{H}{Q} \quad (2)$$

where, A_2 : cross-sectional area of discharge pipe, u_2 : impeller peripheral speed ($= \pi dn$), g : acceleration of gravity, ρ : liquid density, and $H = (p_d - p_s) / (\rho g)$: total head rise across pump.

Before going into the statistical analysis of the measured data, the correlation between input Q and output was checked. Figure 4 shows the coherence function between the flow rate Q , and other variables p_s and p_d with the fluctuation frequency. As can be seen in this figure, the measured values of the coherence function are almost unity within the range of the present experiment, and thus the output p_s and p_d are completely related to the input Q . Figure 5 shows the linearity test result that describes the effect of the magnitude of flow fluctuation $\Delta Q/Q_0$, on the response of total head difference $\Delta H/H_0$. Here ΔQ and Q_0 are magnitude of flow fluctuation and time averaged flow rate, ΔH is the magnitude of the time-dependent total

head difference defined as $(p_d - p_s) / (\rho g)$, H_0 is time averaged total head rise. In this figure, $\Delta H / H_0$ has an amplitude proportional to the rate of flow fluctuation $\Delta Q / Q_0$, and the constant phase shift over the test range of $\Delta Q / Q_0$. Since the $\Delta H / H_0$ is also proportional to $\Delta Q / Q_0$, the above result means that the amplitude and phase correlation between $\Delta H / H_0$ and $\Delta Q / Q_0$ remains constant, indifferent to the magnitude of flow fluctuation. These linearity tests were conducted at all frequencies.

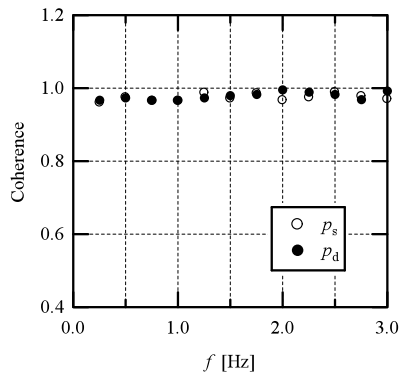


Fig.4 Coherence function between input Q and output p_s and p_d ($\phi_0/\phi_D = 1.0$, $n = 3000 \text{ min}^{-1}$).

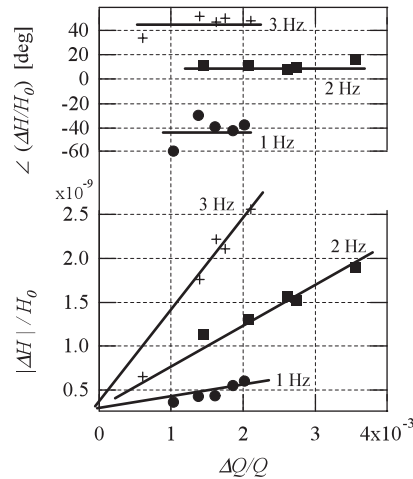


Fig.5 Dependence of the frequency response on amplitude of fluctuations ($\phi_0/\phi_D = 1.0$, $n = 3000 \text{ min}^{-1}$).

5. RESULTS AND DISCUSSIONS

5.1 Static characteristics

Steady state characteristic of the test pump at rotational speed, $n = 2000, 2500$ and 3000 min^{-1} were measured. The total head rise across pump, H , and the flow rate, Q , were made nondimensional using the following relations;

$$\psi = \frac{H}{u_2^2/g} \quad (3)$$

$$\phi = \frac{v_{m2}}{u_2} \quad (4)$$

$$\eta_p = \frac{P_w}{P_M} = \frac{\rho g Q H}{\eta_M P_V} \quad (5)$$

where, d_2 : an outer diameter of rotor, b_2 : passage width, v_{m2} : meridian component of velocity, P_w : hydraulic power, P_M : motor power, P_V : power of motor input, and η_M : motor efficiency.

Figure 6 shows the nondimensional static characteristics of the test pump. The operating point of the test pump was set at the rated condition $\phi_D = 0.03$ ($Q = 7.0 \text{ l/min}$) where η_p , pump efficiency of test pump, reached the maximum value ($\eta_p = 0.14$). As mentioned previously, dynamic characteristics tests were performed both at $\phi = \phi_D$ and $\phi = 0.5\phi_D$.

The whirling motion is an important problem on the test pump with hydrodynamic levitated bearing, CSGB. Figure 7 shows the loci of impeller center at whirling motion in the casing for

various rotational speeds at steady state operation. The eccentricities of the rotor, ε , shift in y direction with increase in rotational speed, while the deviation of the loci of the rotor center, σ , decreases with increasing rotational speeds. Figure 8 shows the standard deviation σ of impeller whirling for various rotational speeds. The σ is bigger for $n < 750 \text{ min}^{-1}$. However, the σ is smaller than the gap between rotor and casing wall surface, and the rotor did not show oscillation. Therefore, the present rotor is stable at steady state operation.

Figure 9 shows whirling ratio of test pump for various rotational speeds. The whirling ratio, Ω/ω , is approximately 0.1 in all rotational speeds as shown in this figure. Suzuki et al. [6] showed that the rotordynamic forces may excite the whirling motion for the region $0 < \Omega/\omega \leq 0.75$. In the present study, however, the rotor does not oscillate, although the whirling ratio is within the range suggested by Suzuki et al. That may be due to the effect of the present CSGB, which generates anti-whirling forces.

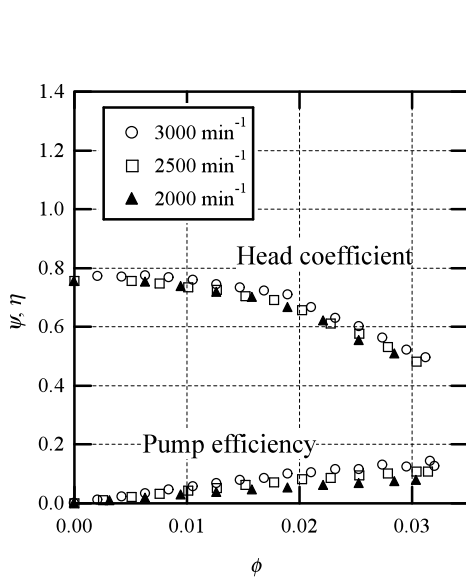


Fig.6 Steady state characteristic curves of test pump.

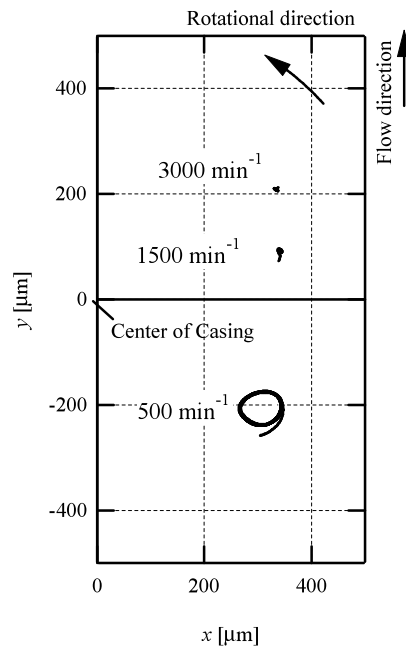


Fig.7 The loci of impeller center for various rotational speeds in steady pump operation; $\phi/\phi_D = 1.0$.

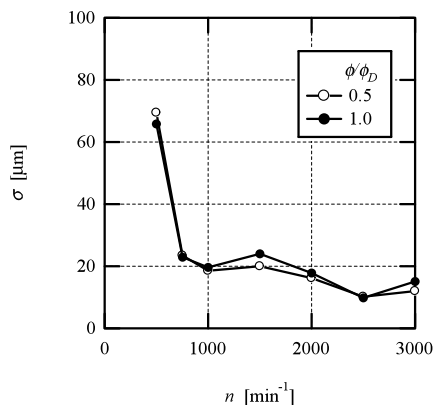


Fig.8 Standard deviation of impeller whirling for various rotational speeds in steady pump operation.

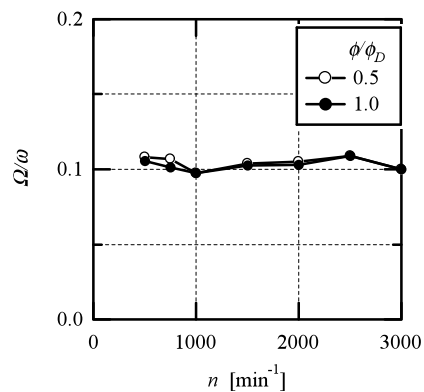


Fig. 9 Whirling ratio of test pump for various rotational speeds in steady pump operation.

5.2 Dynamic characteristics of test pump under flow fluctuations

The pump impeller makes a whirling motion in a casing under unsteady conditions. Figure 10 shows the loci of impeller center under the flow fluctuation at rotational speed $n = 3000 \text{ min}^{-1}$. The eccentricity ε tends to shift toward the pump outlet with increasing fluctuation frequency, whereas the whirling motion increases with increasing fluctuation frequency. These experiments were carried out for the same $\Delta Q/Q_0$, after linearity tests.

Figure 11 shows standard deviations of whirling motion, σ , for various fluctuation frequencies of flow rate. The σ increases with the increasing fluctuation frequency and decreasing impeller rotational speeds. The self-excited vibration does not occur, and thus the present test pump seems to be stable for the range of flow fluctuations in the present study from the rotordynamic point of view.

For the discussion on unsteady characteristics of test pump, Figs. 12 and 13 present the relations of nondimensional pump impedance to fluctuation frequencies for various rotational speeds of pump rotor. Figure 12 shows nondimensional pump resistance $Re(Z_p^*)$ for various fluctuation frequencies of flow rates. Pump resistance increases with increasing fluctuation frequencies at rated condition ($\phi_D/\phi_D = 1.0$), in which pump may be stable because of positive pump resistance. For the frequency $f > 2 \text{ Hz}$ at the low flow rate ($\phi_D/\phi_D = 0.5$), the pump resistance becomes negative, which indicates that pump will be unstable.

The dependence of pump inductance on frequency is shown in Fig. 13, in which the pump inductance tends to increase with frequencies. The pump inductance may increase with frequencies since pump inductance is dependent on the inertia of water in pump. However, the pump inductance shows different tendencies for $f > 1 \text{ Hz}$; $Im(Z_p^*)$ decreases with f at rated conditions, whereas its variations with f are not big at low flow rate. That is because the resistance due to inertia is larger than the viscous drag in the pump, and thus the pump equivalent length decreases with frequencies [14].

Figure 14 shows the pump resistance at fluctuation frequency $f = 1 \text{ Hz}$ ($= 60 \text{ bpm}$) for various rotational speeds. This frequency corresponds to the resting heart rate. Pump resistance does not depend on rotational speed there, and the pump performance tends to shift towards unstable one for lower flow rate. Therefore, special care should be paid for blood pump operation at low discharge.

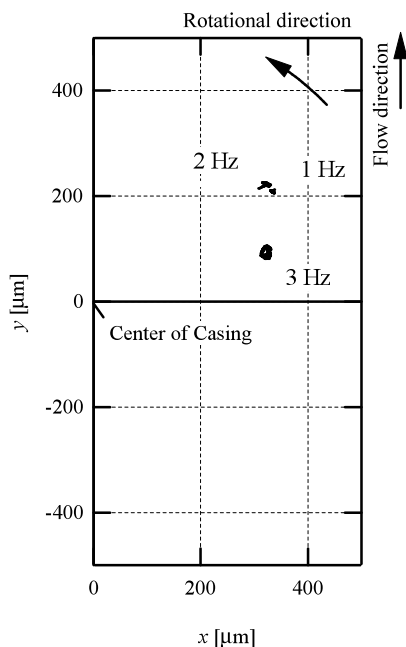


Fig.10 The loci of impeller center for various frequencies under the sinusoidal change in flow rate; $\phi_D/\phi_D = 1.0$, $n = 3000 \text{ min}^{-1}$; $\Delta Q/Q_0 = 0.002$.

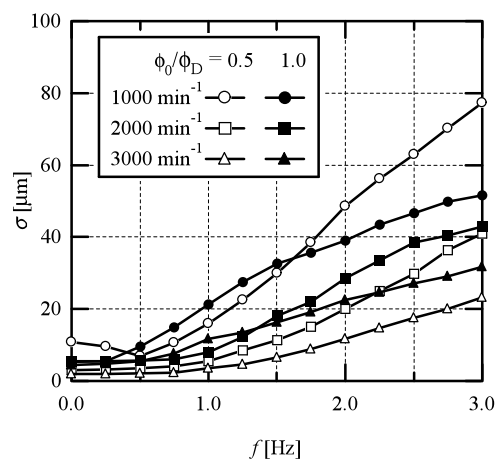


Fig.11 Standard deviation of impeller whirling for various fluctuation frequencies under sinusoidal change in flow rate; $\Delta Q/Q_0 = 0.002$.

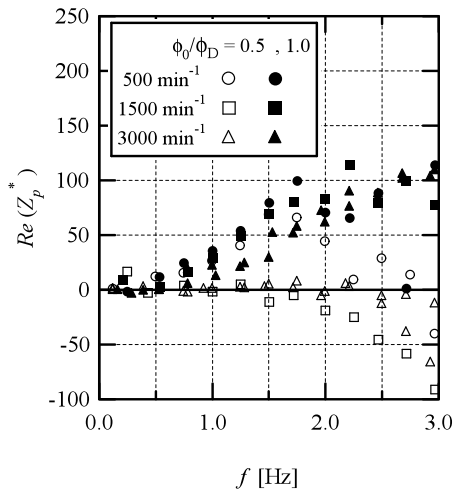


Fig. 12 Nondimensional pump resistance of test pump for various fluctuating frequencies; $\Delta Q/Q_0 = 0.002$.

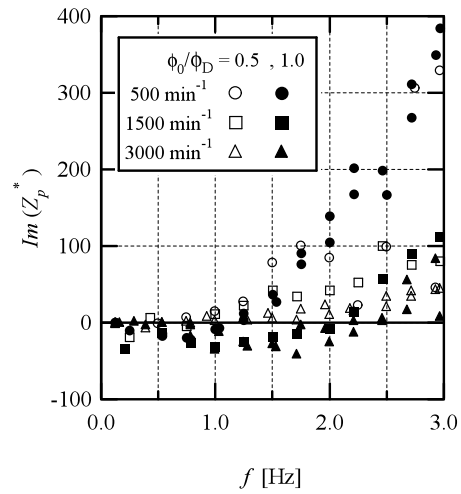


Fig. 13 Nondimensional pump inertia of test pump for various fluctuating frequencies; $\Delta Q/Q_0 = 0.002$

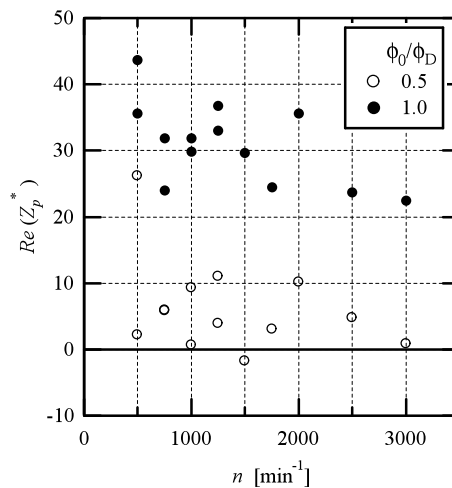


Fig. 14 Pump resistance at $f = 1 \text{ Hz}$ for various rotational speeds; $\Delta Q/Q_0 = 0.002$

6. CONCLUSIONS

The dynamic tests of centrifugal blood pump with conical spiral groove bearings were done under sinusoidal change in flow rates. As the result of the present study, the following conclusions were derived.

- (1) In steady operation, impeller whirling motion decreases with the increasing rotational speed, and thus stable.
- (2) Impeller whirling increases with the increasing fluctuation frequency of flow rate for low rotational speed or low flow rate. The rotational motion of the test pump, however, seems to be stable for the flow fluctuations within the range of the present study.
- (3) At rated condition the pump resistance increases with the increase in fluctuation frequency, and thus the pump is stable. On the other hand, pump resistance falls in negative, and hence the pump

becomes unstable for $f > 2 \text{ Hz}$ at low flow rate ($\phi_o/\phi_D = 0.5$).

(4) At $f = 1 \text{ Hz}$ corresponding to resting heart beat, the pump resistance is small at low flow rate, and thus pump operates near unstable conditions. Therefore, special care should be paid for blood pump operation at low discharge.

ACKNOWLEDGEMENTS

This study was supported by the Grant-in-Aid for Scientific Research from Japan Society for the Promotion of Science (Scientific Research B 20360086). We are also grateful to Mr. Yuki Tsuruta for his contribution to this study.

REFERENCES

- [1] Yoshino, Y., and Akamatsu, T., Performance and Characteristics of Magnetically Suspended Centrifugal Blood Pump, *Trans. JSME, Ser. B*, 1994, 60(579), 3687-3692.
- [2] Asama, J., Shinshi, T., Hoshi, H., Takatani, S., and Shimokohbe, A., A Compact Highly Efficient and Low Hemolytic Centrifugal Blood Pump with a Magnetically Levitated Impeller, *Artificial Organs*, 2006, 30(3), 160-167.
- [3] Asama, J., Shinshi, T., Hoshi, H., Takatani, S., and Shimokobe, A., Dynamic Characteristics of a Magnetically Levitated Impeller in a Centrifugal Blood Pump, *Artificial Organs*, 2007, 31(4), 301-311.
- [4] Ochiai, Y., Golding, L., Massiello, A., Medvedev, A., Gerhart, R., Chen, J., Takagi, M., and Fukamachi, K., In Vivo Hemodynamic Performance of the Cleveland Clinic CorAide Blood Pump in Calves, *The Annual Thoracic Surgery*, 2001, 72, 747-52.
- [5] Chung, M., Zhang, N., Tansley, G., and Qian, Y., Experimental Determination of Dynamic Characteristics of the VentrAssist Implantable Rotary Blood Pump, *Artificial Organs*, 2004, 28(12), 1089-1094.
- [6] Suzuki, T., Prunieres, R., Horiguchi, H., Tsukiya, T., Taenaka, Y., and Tsujimoto, Y., The Rotordynamic Fluid Forces on an Artificial Heart Pump Impeller in Whirling Motion, *Trans. JSME, Ser. B*, 2007, 73(725), 205-212.
- [7] Brennen, C., Hydrodynamics of pumps, Concepts ETL, Inc., 1994.
- [8] Anderson, D.A., Blade, R.J., and Stevans, W., Response of a Radial-Bladed Centrifugal Pump to Sinusoidal Disturbances for Noncavitating Flow, NASA TN D-6556, 1971.
- [9] Ng, S.L., and Brennen, C., Experiments on the Dynamic Behavior of Cavitating Pumps, *Trans. ASME, J. Fluids Eng.*, 1978, 100, 166-176.
- [10] Nakamura, Y., Tsukamoto, H., Miyazaki, K., and Qian, Y., Experimental study of Dynamic Characteristics of a Centrifugal Blood pump with a Conical Spiral Groove Bearing for a Ventricular Assist Device, *5th Joint ASME / JSME Fluids Engineering Conference*, 2007, FEDSM2007-37235.
- [11] Muijderman, E.A., Analysis and design of Spiral-Groove Bearings, *ASME J. Lubric. Tech.*, 1967, 89, 291-306.
- [12] Tsukamoto, H., Yoneda, H., and Sagara, K., The Response of a Centrifugal Pump to Fluctuating Rotational Speed, *Trans. ASME J. Fluids Eng.*, 1995, 117, 489-484.
- [13] Kawata, Y., Ebara, K., Uehara, S., and Takata, T., System Instability Caused by the Dynamic Behaviour of a Centrifugal Pump at Partial Operation, *JSME International Journal*, 1987, 30(260), 271-278.
- [14] Sano, M., Pressure Pulsation in Turbo-Pump Piping System (1st Report, Experiments on the Natural Frequencies of the Liquid Column of Centrifugal Pump Piping Systems), *Trans. JSME, Ser. B*, 1983, 49(440), 828-836.